



## Florida Straits density structure and transport over the last 8000 years

Jean Lynch-Stieglitz,<sup>1</sup> William B. Curry,<sup>2</sup> and David C. Lund<sup>3</sup>

Received 11 November 2008; revised 5 May 2009; accepted 24 June 2009; published 1 September 2009.

[1] The density structure across the Florida Straits is reconstructed for the last 8000 years from oxygen isotope measurements on foraminifera in sediment cores. The oxygen isotope measurements suggest that the density contrast across the Florida Current increased over this time period. The magnitude of this change corresponds to an increase in the geostrophic transport referenced to 800 m water depth of 4 sverdrups (Sv) over the last 8000 years. The spatial and seasonal distribution of incoming solar radiation due to changes in the Earth's orbit has caused systematic changes in the atmospheric circulation, including a southward migration of the Intertropical Convergence Zone over the last 8000 years. These changes in atmospheric circulation and the associated wind-driven currents of the upper ocean could readily account for a 4 Sv increase in the strength of the Florida Current. We see no evidence in our data for dramatic changes in the strength of the Atlantic Meridional Overturning Circulation over this time period.

**Citation:** Lynch-Stieglitz, J., W. B. Curry, and D. C. Lund (2009), Florida Straits density structure and transport over the last 8000 years, *Paleoceanography*, 24, PA3209, doi:10.1029/2008PA001717.

### 1. Introduction

[2] The Florida Current, the portion of the Gulf Stream that passes through the Florida Straits, transports 28–32 sverdrups (Sv) of water. Some of this water (about 13 Sv) comes from the South Atlantic, entering the Caribbean through its southernmost passages [*Schmitz and Richardson*, 1991]. This cross-equatorial flow compensates the southward flow of North Atlantic Deep Water (NADW), and represents the northward flowing surface branch of the Atlantic Meridional Overturning Circulation (AMOC). The remaining flow (about 17 Sv) is driven by the winds, entering the Caribbean through a variety of passages, and including the final additions to the Florida Current through the Old Bahama Channel and Northwest Providence Channel at the Bahamas [*Johns et al.*, 2002; *Schmitz et al.*, 1992] (Figure 1). Long-term monitoring of the Florida Current at 27°N shows seasonal, interannual and decadal fluctuations with a total amplitude of 4–5 Sv which appear to reflect changes in the large-scale atmospheric circulation over these timescales [*Baringer and Larsen*, 2001]. We can expect that these fluctuations persisted throughout the Holocene together with variability on longer timescales (centennial to multi-millennial), which can be uncovered by extending the observational record into the past.

[3] There appears to be significant variability in atmospheric and Atlantic ocean circulation on millennial timescales, possibly linked to changes in solar output [*Bond et al.*,

2001; *deMenocal et al.*, 2000; *Hall et al.*, 2004; *Oppo et al.*, 2003]. The most recent of these millennial-scale oscillations, linked to the “Little Ice Age” cooling in Europe, appears to be associated with small changes in the Florida Current [*Lund et al.*, 2006], and it seems possible that some of these earlier millennial-scale changes in the ocean-climate system might also be linked to changes in the Florida Current.

[4] There has been a trend of decreasing seasonality of incoming solar radiation in the Northern Hemisphere over the Holocene, linked to dramatic changes in precipitation. The Sahara and Sahel have dried considerably over the last 8 ka [*Gasse*, 2000; *Hoelzmann et al.*, 1998] and there appears to have also been a southward shift of the Intertropical Convergence Zone (ITCZ) over this time period in the Western Atlantic [*Haug et al.*, 2001]. It is certainly plausible that the associated changes in atmospheric circulation could have resulted in variability of the wind-driven transport through the Florida Straits. The early to mid-Holocene was also a time of extreme warmth in the North Atlantic and Northern Hemisphere [*Kaufman et al.*, 2004; *Marchal et al.*, 2002]. A strong early Holocene AMOC, due to a stronger southward flow of NADW and compensating return flow of surface and intermediate waters, has been invoked as a possible mechanism for amplifying the high-latitude warming [*Kerwin et al.*, 1999]. While it is not possible to strictly separate the portion of the Florida Current associated with the surface branch of the AMOC from the total flow, it seems reasonable to expect that a dramatic strengthening or weakening of the AMOC will be associated with changes in the density structure and flow through the Straits.

[5] We have previously shown that the shear in the geostrophic transport through the Florida Straits can be reconstructed for times in the past using oxygen isotope measurements on benthic foraminifera as a proxy for seawater density [*Lynch-Stieglitz et al.*, 1999a, 1999b]. Using this approach, *Lund et al.* [2006] inferred Florida Current

<sup>1</sup>School of Earth and Environmental Sciences, Georgia Institute of Technology, Atlanta, Georgia, USA.

<sup>2</sup>Woods Hole Oceanographic Institution, Woods Hole, Massachusetts, USA.

<sup>3</sup>Department of Geological Sciences, University of Michigan, Ann Arbor, Michigan, USA.

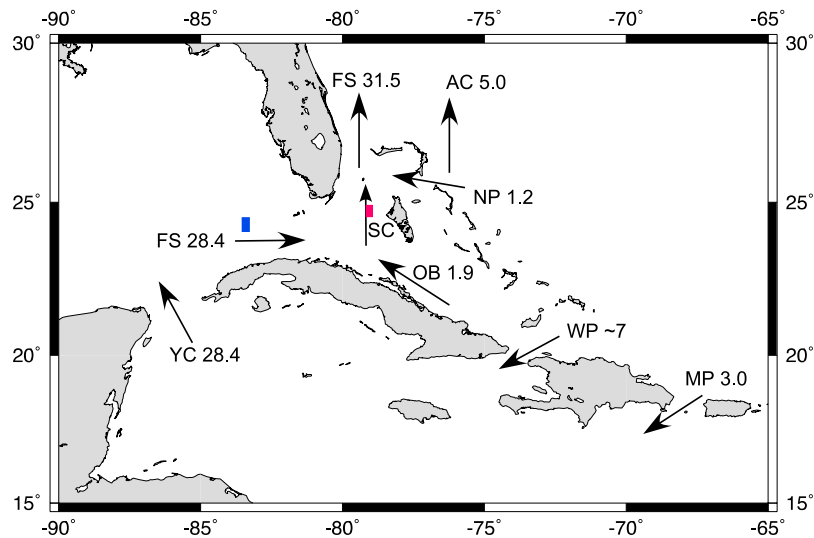


**Figure 1.** Location of sediment cores in the Florida profile (blue box) and the Bahamas profile (red box). Also indicated are the transports (in Sv) through the Florida Straits (FS), Yucatan Channel (YC), Mona Passage (MP), Windward Passage (WP), Old Bahama Channel (OB), Northwest Providence Channel (NP), and the Antilles Current (AC). The location of the Santaren Chanel (SC) is also indicated. Transports are from *Johns et al.* [2002].

variability over the last 1000 years, finding that it was of a similar magnitude ( $<4$  Sv total amplitude) as modern interannual and decadal variability. This variability was linked to large-scale climate changes in the Northern Hemisphere. Here we quantitatively assess variability in the Florida current over the last 8000 years B.P. at millennial time resolution using the same approach. This time period is characterized by relatively constant ice volume and carbon dioxide, so that trends in Florida Current strength can be used to assess the sensitivity of ocean circulation and climate to changing distribution and seasonality insolation over the Holocene.

## 2. Material and Methods

[6] With two vertical profiles of seawater density on either side of the Florida current, we can reconstruct the vertical shear in the geostrophic transport. We construct our vertical density profiles, and extend them back in time using a series of sediment cores at various water depths along the Florida margin on the landward side of the current, and on the Great Bahama Bank on the seaward side (Figure 1). The cores are dated using  $^{14}\text{C}$  measurements on planktonic foraminifera, and seawater density at each core depth is estimated from the oxygen isotope ratio of the calcite tests of benthic foraminifera. Density for the surface mixed layer is estimated using oxygen isotope ratios in planktonic foraminifera. The oxygen isotopic composition of the foraminifera reflects the temperature of calcification and the oxygen isotopic composition of seawater, which is correlated to seawater salinity in midlatitude surface waters and in the main thermocline of the ocean [*Craig and Gordon*, 1965]. At a given depth, seawater density is controlled by temperature and salinity, resulting in a tight regional correlation between seawater density

and  $\delta^{18}\text{O}$  of benthic foraminifera [*Lynch-Stieglitz et al.*, 1999a].

[7] In January of 2002, we collected a series of piston, gravity and multicore at water depths from 200 to 750 m on the Florida margin near Dry Tortugas Key and on the Great Bahama Bank (Figure 1 and Table 1). Benthic foraminifera were picked from the  $>250\ \mu\text{m}$  size fraction of the sediments for oxygen isotope analysis. We analyzed groups of three individuals of *Cibicides pachyderma* where they were available. In some cases, fewer were analyzed, and in some cores we also analyzed *Planulina ariminensis* and *Planulina wuellerstorfi* in order to generate more complete time series. Previous studies in this region have not shown any offset in the oxygen isotope composition of these species [*Lynch-Stieglitz et al.*, 1999a; *Slowey and Curry*, 1995]. In order to constrain mixed layer properties, the planktonic foraminifera *Globogerrinoides sacculifer* without sac-like chamber was picked from the 355–425  $\mu\text{m}$  size fraction of the sediments for one core in each transect. The *G. sacculifer* were analyzed in groups of 8 individuals. Oxygen isotope analyses were made at Lamont-Doherty Earth Observatory using a Micromass Optima with Multi-prep carbonate preparation device and at Woods Hole Oceanographic Institution on a Finnigan MAT252 and MAT253 with Kiel carbonate device. All instruments were calibrated via NBS-19 and NBS-18 standards, with a long-term precision of replicate NBS-19 and in-house standards of  $<0.08\ \text{‰}$  for all systems. Some replicate analyses were run at both locations to determine whether there were any systematic interlaboratory offsets, and none were found.

[8] We picked planktonic foraminifera for accelerator mass spectrometry (AMS) radiocarbon dates at depths in the cores where we observed significant changes in the oxygen isotopic composition of the benthic foraminifera, for an average of 6 dates for each core over the last 10,000 years

**Table 1.** Core Locations and Data Summary

Core	Water Depth (m)	Latitude	Longitude	Species Analyzed	Data Source
<i>Florida Profile</i>					
Knr166-2 1GGC	446	24°23.06N	83°20.27W	<i>G. sacculifer</i>	this study
Knr166-2 2JPC	446	24°23.05N	83°20.32W	<i>G. sacculifer</i>	this study
Knr166-2 50MC	198	24°24.70N	83°13.14W	<i>C. pachyderma</i>	Lund et al. [2006]
Knr166-2 49GGC	198	24°24.70N	83°13.14W	<i>C. pachyderma</i>	Lund et al. [2006]
Knr166-2 51JPC	198	24°24.70N	83°13.14W	<i>C. pachyderma</i>	this study
Knr166-2 16MC	248	24°23.72N	83°13.53W	<i>C. pachyderma</i>	Lund et al. [2006]
Knr166-2 48JPC	247	24°23.73N	83°13.53W	<i>C. pachyderma</i>	this study
Knr166-2 59JPC	358	24°25.05N	83°22.09W	<i>C. pachyderma</i>	this study
Knr166-2 3MC	447	24°23.04N	83°20.33W	<i>C. pachyderma</i> , <i>P. ariminensis</i>	Lund et al. [2006]
Knr166-2 1GGC	446	24°23.06N	83°20.27W	<i>C. pachyderma</i> , <i>P. ariminensis</i>	this study
Knr166-2 2JPC	446	24°23.05N	83°20.32W	<i>C. pachyderma</i> , <i>C. sp.</i>	this study
Knr166-2 62MC	547	24°19.60N	83°15.40W	<i>C. pachyderma</i> , <i>P. ariminensis</i>	Lund et al. [2006]
Knr166-2 8GGC	546	24°19.60N	83°15.14W	<i>C. pachyderma</i>	this study
Knr166-2 26JPC	546	24°19.61N	83°15.14W	<i>C. pachyderma</i>	this study
W167-79GGC	530	24°21.50N	83°20.90W	<i>C. pachyderma</i> , <i>P. ariminensis</i>	Lund et al. [2006]
Knr166-2 27GGC	598	24°18.65N	83°15.37W	<i>C. pachyderma</i>	this study
Knr166-2 29JPC	648	24°16.93N	83°16.24W	<i>C. pachyderma</i>	this study
Knr166-2 11MC	751	24°13.18N	83°17.75W	<i>C. pachyderma</i> , <i>C. sp.</i>	Lund et al. [2006]
Knr166-2 31JPC	751	24°13.18N	83°17.75W	<i>C. pachyderma</i> , <i>P. wuellerstorfi</i>	Came et al. [2007], this study
<i>Bahamas Profile</i>					
Knr166-2 73GGC	542	23°44.73N	79°25.78W	<i>G. sacculifer</i>	this study
Knr166-2 105JPC	304	24°33.83N	79°13.77W	<i>C. pachyderma</i>	this study
Knr166-2 106JPC	354	24°33.77N	79°14.14W	<i>C. pachyderma</i>	this study
Knr166-2 113JPC	402	24°38.47N	79°14.21W	<i>C. pachyderma</i> , <i>C. sp.</i>	this study
Knr166-2 134MC	441	24°50.16N	79°13.11W	<i>C. pachyderma</i>	Lund et al. [2006]
Knr166-2 135JPC	446	24°50.15N	79°13.12W	<i>C. pachyderma</i>	this study
Knr166-2 118MC	531	24°35.43N	79°16.12W	<i>C. pachyderma</i>	Lund et al. [2006]
Knr166-2 117GGC	528	24°35.44N	79°16.12W	<i>C. pachyderma</i>	Lund et al. [2006]
Knr166-2 119JPC	529	24°35.43N	79°16.12W	<i>C. pachyderma</i>	this study
Knr166-2 127JPC	631	24°45.83N	79°15.94W	<i>C. pachyderma</i>	this study
Knr166-2 132JPC	739	24°50.90N	79°16.88W	<i>C. pachyderma</i> , <i>P. ariminensis</i> , <i>C. sp.</i>	this study

(Data Set S1).<sup>1</sup> Most dates were on the mixed layer dwelling species *Globigerinoides ruber* and/or *Globigerinoides sacculifer*. All radiocarbon measurements were made at the National Ocean Sciences AMS facility in Woods Hole, and were corrected using Calib 5.0.2 (M. Stuiver et al., 2005; available at <http://calib.qub.ac.uk/calib/>) using the standard marine reservoir correction [Hughen et al., 2004]. Age models were constructed by linearly interpolating between the radiocarbon control points. Holocene sedimentation rates were variable and ranged from 8 to 70 cm ka<sup>-1</sup> on the Florida Margin and 60 to 370 cm ka<sup>-1</sup> for the Bahamas, with the lower sedimentation rates in deeper water in both locations.

[9] We then averaged the oxygen isotope data into 1000 year bins, with bins centered every 500 years. The averaging interval was chosen to include sufficient number of analyses for a robust estimate for the cores with the lowest sedimentation rates. We also include in these averages the benthic foraminifera  $\delta^{18}\text{O}$  data presented by Lund et al. [2006] which provides greater data density for the last 2000 years. The 1000 year bins contained between 2 and 396 analyses, with an average of 22 analyses per bin.

[10] Vertical profiles were constructed at each time interval by first linearly interpolating the average  $\delta^{18}\text{O}$  of the benthic foraminifera between core depths. Before 6 ka B.P. the core depths were corrected for the sea level changes associated with the melting of the continental ice sheets [Lambeck and Chappell, 2001]. The averages from the planktonic foraminifera,

*G. sacculifer*, were used to reconstruct properties in the surface mixed layer. *G. sacculifer* is a spinose foraminifera which bears photosynthetic symbionts. While it lives mainly in the euphotic zone it adds some calcite at depth late in its life cycle [Bé, 1980]. There is no direct information about the seasonality of this species in this region. The waters overlying the core sites are oligotrophic year-round, with maximum productivity during the winter months [González et al., 2000] which might tend to bias the isotopic record from the foraminifera toward wintertime conditions. However, *G. sacculifer* seems well adapted for low-nutrient conditions and is most tolerant of warm surface temperatures which might tend to bias the specimens in the sediments toward summer time conditions as it does in the Sargasso Sea [Deuser and Ross, 1989]. The isotopic composition of *G. sacculifer* in the most recent sediments indicates that this species is currently recording mean annual conditions in this region. The mixed layer depth was fixed at 100 m, which is near the modern winter time value in this area (75–100 m) [Kara et al., 2002] and consistent with the CTD data from near the core sites (Figure 2). For the Florida Margin profile, the  $\delta^{18}\text{O}$  is linearly interpolated between the bottom of the mixed layer and the shallowest sediment core. Because of the extremely high Holocene sedimentation rates, we were not able to obtain cores above 300 m water depth at the Bahamas with full coverage of the last 8 ka. Today, the relatively homogeneous properties of the subtropical mode waters extend from about 450 to 250 m water depth (Figure 2). In order to better capture this structure, for the Bahamas profile we extrapolate the  $\delta^{18}\text{O}$  from the

<sup>1</sup>Auxiliary material data sets are available at <ftp://ftp.agu.org/apend/pa/2008pa001717>. Other auxiliary material files are in the HTML.

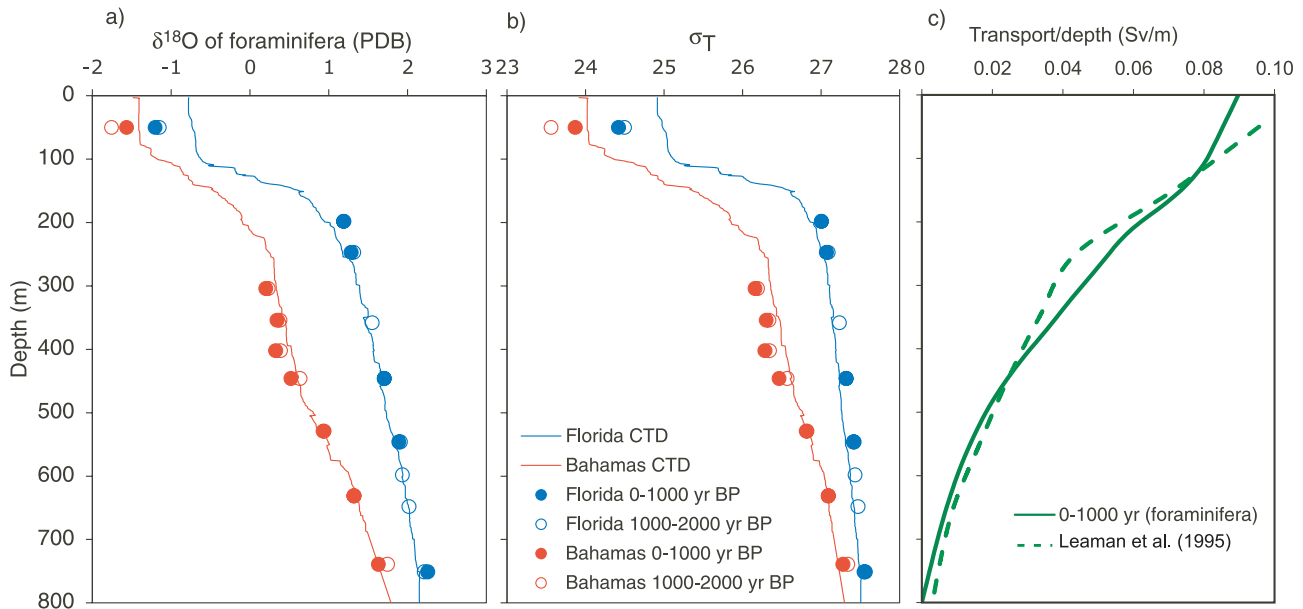


**Figure 2.** (a) Average oxygen isotope ratios from benthic foraminifera (*Cibicidoides* and *Planulina*) for 0–1000 years (open symbols) and 1000–2000 years (closed symbols). Also shown at 50 m water depth are the values for the planktonic foraminifera *G. sacculifer* which is assumed to calcify in the surface mixed layer. Data from the Florida cores are indicated in blue, and data from the Bahamas are indicated in red. Also shown is the isotopic composition of foraminifera predicted from seawater temperature and salinity measurements from CTD casts taken in January 2002. (b) The oxygen isotope ratios in Figure 2a converted to density ( $\sigma_T$ ). Also shown is the density calculated from the CTD casts. (c) Calculated geostrophic transport per unit depth (dark green) and observed transport from the Florida Straits and Santaren Channel from *Leaman et al.* [1995] (light green).

shallowest core up to a depth of 250 m (top of the mode water). We then linearly interpolate between 250 m and the base of the mixed layer. The values for the deepest core in each transect were extrapolated to the 800 m reference level.

[11] For 0–6 ka B.P., density is then calculated from the foraminiferal  $\delta^{18}\text{O}$  using the empirical relationship for waters in today’s subtropical North Atlantic [*Lynch-Stieglitz et al.*, 1999a]:

$$\sigma_T = 25.951 + 1.0771\delta^{18}\text{O} - .016055\delta^{18}\text{O}^2$$

We are assuming that the factors influencing this relationship (the relationship between temperature, salinity and  $\delta^{18}\text{O}$  of water ( $\delta^{18}\text{O}_w$ ) in the main thermocline) are relatively constant over this time period. The relationship between  $\delta^{18}\text{O}_w$  and salinity in midlatitude to high-latitude surface waters (and thus also in the thermocline) is almost linear, and suggests a mixture between an oceanic end-member and a fresh end-member corresponding to midlatitude precipitation [*Craig and Gordon*, 1965]. The  $\delta^{18}\text{O}_w$  in the ice accumulating on Greenland is remarkably stable over the Holocene with a total range of less than 2 ‰ [*Andersen et al.*, 2004], arguing for a relatively constant  $\delta^{18}\text{O}_w$  of the high-latitude precipitation end-member for the last 10,000 years. However, the salinity and  $\delta^{18}\text{O}_w$  of the deep ocean were still decreasing because of the melting of the continental ice sheets between 8 and 6 ka B.P. For this time interval we recompute the expected relationship between the  $\delta^{18}\text{O}$  of foraminifera and

density by taking the modern T-S- $\delta^{18}\text{O}_w$  data from this region, increasing the S and  $\delta^{18}\text{O}$  by a uniform amount for each time interval. The size of the shift is determined using the sea level data by *Lambeck and Chappell* [2001] and a whole ocean change in  $\delta^{18}\text{O}_w$  of 1.05 ‰ per 140 m of sea level change [*Schrag et al.*, 2002]. This ice volume correction in the density relationship makes a maximum difference of +2 Sv at 8 ka B.P. in the flow calculations relative to the calculation assuming the modern relationship.

[12] Once the  $\delta^{18}\text{O}$  profiles are converted to density, the geostrophic transport and the vertical distribution of the transport are computed. We treat the profiles as two vertical density profiles, assign a zero velocity at a reference level of 800 m, and use the geostrophic method to calculate transport. The locations of the depth transects, on either side of the Florida Current, were chosen because they are areas where sediments accumulate. Many of the modern observations of Florida Straits transport have focused on the more constricted portions of the Florida Straits where sediments are not accumulating because of the strong bottom currents. While the two profiles do not define a section perpendicular to the axis of the flow, this is not necessary for the calculation of the geostrophic transport across the section. The two density profiles are also not truly vertical (they represent the density along the slope), which invalidates the assumption of hydrostatic balance that goes into the calculation of geostrophic shear. However, by necessity, our cores are collected in areas where the near bottom currents are relatively weak and where

the sediments can accumulate. Thus, our profile along the slope closely approximates a vertical profile in a nearby area offshore where the hydrostatic balance does hold. There are changes in the vertical structure of the Florida Current between the Southern Straits (near the Florida Keys core transect) and at 25°N opposite the Bahamas core transect. Reflecting this, the density along the boundaries of the Florida Straits changes along the flow path as well. Some of these differences result from the additional flow that joins the Florida Current through the Old Bahama Channel and some are due to the complex bathymetry in this region. We will show that, despite these complications, it is possible to reconstruct a vertical structure of the transport through the Florida Straits that is fairly consistent with the structure observed in the modern instrumental record. More sophisticated methods of combining the dynamical theory and models with the data (e.g., inverse methods) to reconstruct flow may improve the accuracy of transport estimates, but are beyond the scope of this work.

[13] Our choice of a reference level at 800 m is based on the fact that free-falling current profiler data from the Southern Straits (near the Florida Keys cores) indicate that the flow is small at this depth [Leaman *et al.*, 1995] (Figure 2) and that our deepest core in the Bahamas profile is limited by the bathymetry to 740 m water depth. The velocity in the Southern Florida Straits (near the Florida profile) at 800 m is about  $7 \text{ cm s}^{-1}$  [Leaman *et al.*, 1995] which would lead to an underestimation of flow by 3.5 Sv using an 800 m level of no motion (this number is obtained by multiplying the velocity by the area of the section). The flow in the shallower Northern part of the Florida Straits (near the Bahamas profile) is very small at the bottom [Leaman *et al.*, 1989], and a level of no motion at 800 (approximately the bottom of the channel) would give an accurate geostrophic transport across the Straits. Presumably, the error introduced by using an 800 m level of no motion with our sediment core profiles is somewhere in between these two cases (an underestimate of <3.5 Sv). There is no physical reason that the vertical structure of the velocity is constant with time and the calculated velocities shown here are only accurate to the degree the velocity at 800 m remains small throughout the last 8 ka.

[14] We assess impact of uncertainties in the  $\delta^{18}\text{O}$  values used in the transport calculation using Monte Carlo simulations as by Lund *et al.* [2006]. For each time interval, a  $\delta^{18}\text{O}$  value is randomly sampled for each core given the mean and standard error. Then the oxygen isotope values are interpolated, converted to density and the geostrophic transport calculated as described above. This is done 100 times in order to determine the mean and standard deviation of the transport estimate for each time interval. While the error in the transport estimate varies with time (the errors are lower when larger numbers of analyses within each time interval contribute to a smaller standard error), on average the  $2 - \sigma$  error is  $\pm 1.1 \text{ Sv}$ .

### 3. Results and Discussion

#### 3.1. Late Holocene Transport

[15] The average oxygen isotope values for the most recent (0–2 ka) time intervals compare well to the structure

predicted on the basis of modern water column measurements and the independently generated paleotemperature equation for *Cibicidoides* and *Planulina* species [Lynch-Stieglitz *et al.*, 1999a] (Figure 2a). The computed seawater density values, based on this same relationship, reflect values calculated from measured temperature and salinity (Figure 2b). The foraminifera values are slightly denser (higher  $\delta^{18}\text{O}$ ) than the water column values on the Florida margin, and slightly less dense (lower  $\delta^{18}\text{O}$ ) in the subtropical mode waters of the Bahamas profile. At this point it is difficult to say whether this is because there is some small error in the paleotemperature equation, some uncertainty in the estimate of seawater  $\delta^{18}\text{O}$ , or simply that the conditions in January 2002 (the time of the water column measurements) do not reflect the long-term average conditions over the last 2000 years. Planktonic foraminifera, which are assumed to reflect average annual conditions, are used to determine the mixed layer  $\delta^{18}\text{O}$  and density. These values are, as expected, different from the water column mixed layer conditions which were measured on a single day during the winter.

[16] The mean of Florida Straits transport at 27°N is now well established by a number of different observational methods to be  $31.5 \pm 1.5 \text{ Sv}$  [Lee *et al.*, 1996]. However, our profiles on the Great Bahama Banks and the Florida margin will measure the Florida Straits transport before the final addition of waters through the Northwest Providence Channel. The magnitude of the additional flow contributed through the Northwest Providence Channel is not well constrained [Johns *et al.*, 2002]. Leaman *et al.* [1995] found a mean transport of 1.2 Sv into the Florida Straits on three different cruises in 1990 and 1991 with a range from  $-1.1 \text{ Sv}$  to 2.9 Sv. If the mean flow is close to 1.2 Sv, we would expect to measure a modern transport between the location of our core transects of 30.3 Sv ( $31.5 - 1.2$ ). However, given the range in values and small number of measurements, the true mean value could be several Sv higher or lower than this value. The value we calculate from the benthic foraminifera for 0–1000 years B.P.,  $29.7 \pm 0.9$  ( $2 - \sigma$  error) is the same as observed modern average transport within the uncertainties of both approaches (Figure 2c).

#### 3.2. Millennial Resolution Flow Reconstruction

[17] Both core transects show a decrease in foraminiferal  $\delta^{18}\text{O}$  at all water depths from 8 ka B.P. to the present (Figures 3a and 3b). The largest changes (0.3 ‰ over 8 ka) are in the cores that sample the subtropical mode water on the Bahamas side (Knorr 166-2 106JPC and 135JPC) compared with less than 0.1‰ on the Florida side. The density calculated from these  $\delta^{18}\text{O}$  measurements also, not surprisingly, decreases toward the present (Figures 3e and 3f). However, the inferred density decrease is stronger for the Bahamas profile than for at the same depth in the Florida profile, which leads to an increase in the horizontal density gradient across the Florida Current. The geostrophic flow calculated on the basis of this increasing density gradient and the assumption of an unchanging reference level increases with time by about 4 Sv over the last 8 ka (Figure 4).

[18] Some of the decrease foraminiferal  $\delta^{18}\text{O}$  and inferred density for both profiles is due to the input of isotopically

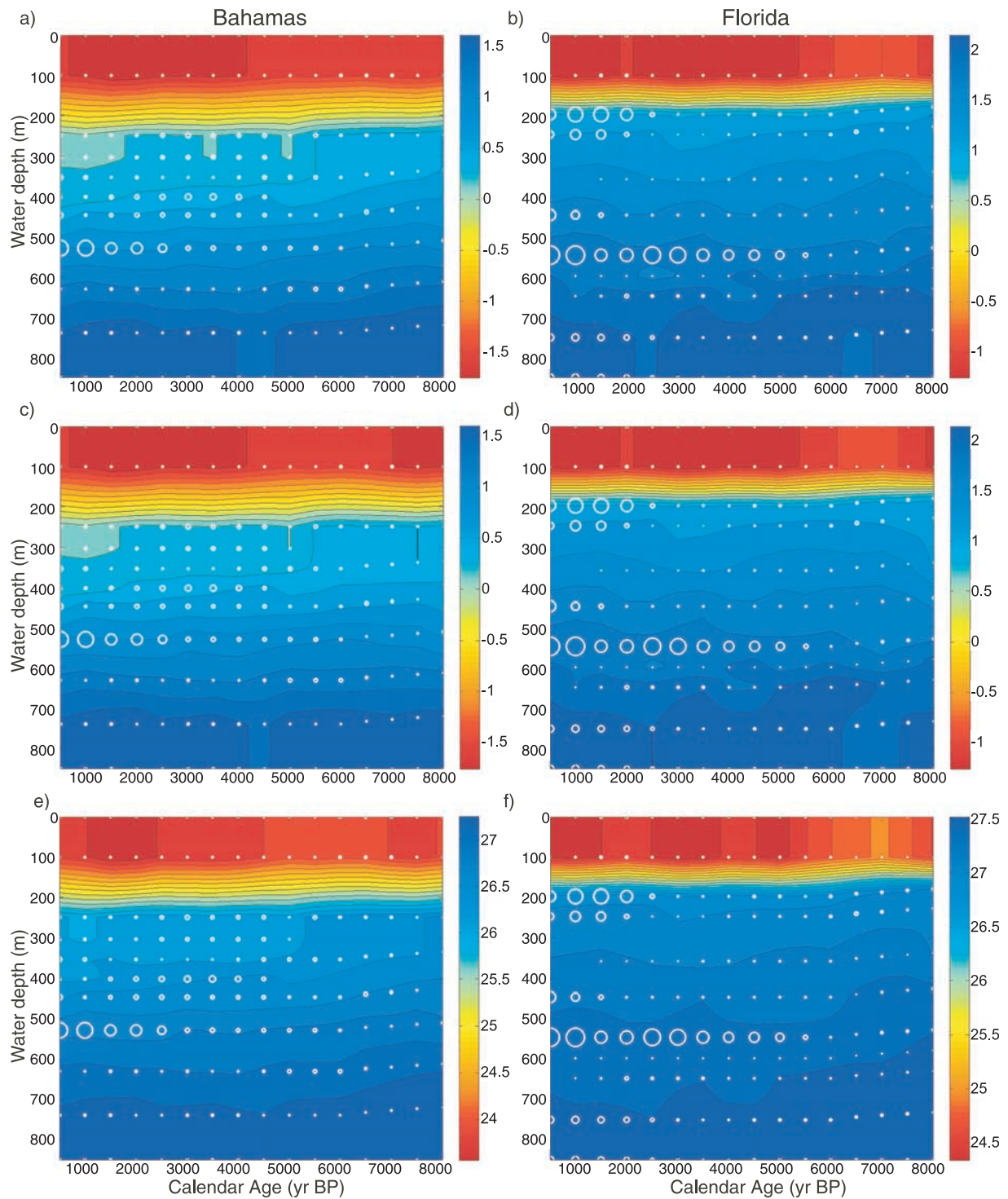


**Figure 3.** The 1000 year averaged oxygen isotope ratios (‰, PDB) for (a) the Bahamas profile and (b) the Florida profile. The averaged oxygen isotope ratios corrected for the whole ocean changes between 6 and 8 ka B.P. for (c) the Bahamas and (d) the Florida profiles. The density estimates ( $\sigma_T$ ) for the (e) Bahamas and (f) Florida profiles. The positions of the white circles represent the depth for which we have data at each time interval. The area of the white circle represents the number of individual foraminifera analyzed for the average at each of these depths. The markers at the top and bottom of the surface mixed layers represent data from the measurements on planktonic foraminifera for each profile which is assumed to be representative of the entire mixed layer. For the Bahamas profile, the markers at 250 m water depth represent the extrapolation of the shallowest benthic data to the top of the mode water. All other markers represent measurements on benthic foraminifera from a single sediment core.

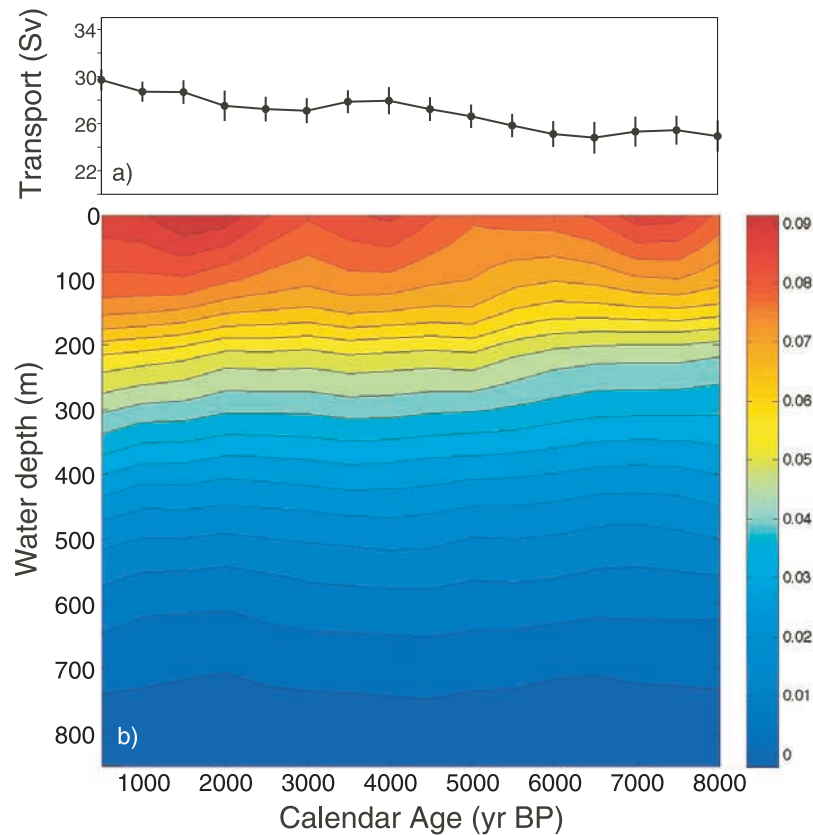


**Figure 4.** (a) Calculated geostrophic transport through the Florida Straits with  $2 - \sigma$  error estimates. (b) Geostrophic transport per unit depth ( $\text{Sv m}^{-1}$ ).

light water into the ocean from the final demise of the Northern Hemisphere ice sheets. Once the component of the  $\delta^{18}\text{O}$  due to global ice volume is removed, we still see a gradual decrease in foraminiferal  $\delta^{18}\text{O}$  in the Bahamas profile, especially at the depths of the Subtropical Mode Water (Figure 3c). It is this decrease in mode water  $\delta^{18}\text{O}$  that is largely driving the increase in flow calculated over the last 8 ka.

[19] It is possible that there is centennial-scale variability in flow over the last 8 ka on the order of 2–4 Sv, just as there appears to be over the last 1000 years [Lund *et al.*, 2006]. However, to reconstruct centennial-scale variability would require higher temporal resolution in measurements of foraminiferal  $\delta^{18}\text{O}$  and radiocarbon than we present in this study.

### 3.2.1. Atlantic ITCZ Changes

[20] Both modeling results [Braconnot *et al.*, 2007] and data-based studies [Haug *et al.*, 2001] suggest a migration of the ITCZ to the south over this time period. In the models, this shift is ultimately driven by the decrease in seasonality due to the precessional cycle. The impact of the atmospheric circulation change associated with this southward shift of the ITCZ on the wind-driven flow through the Florida Straits will be determined by the change in the Sverdrup transport at the Windward Passage [Johns *et al.*, 2002; Schmitz *et al.*, 1992]. Today the Sverdrup transport at the Windward Passage, which is proportional to the north-south shear in the zonal wind stress across the Atlantic basin

at this latitude, matches the approximately 13 Sv of the modern Florida Straits transport that enters the Caribbean as part of the wind-driven subtropical gyre. It is difficult to evaluate precisely how a shift in the ITCZ alone would impact the wind stress shear at this latitude.

[21] In an idealized climate model simulation in which the ITCZ is shifted to the south by imposed heat flux anomalies, Broccoli *et al.* [2006] show wind fields that would suggest increased Sverdrup transport at the Windward passage, and thus an increase in the wind-driven transport through the Florida Straits. We can estimate the potential magnitude of the change in the wind-driven flow by examining today's wind field and wind-driven circulation. Today the Sverdrup transport approximately 2.5 degrees north of the Windward Passage is about 4 Sv greater than at the latitude of the Windward Passage [Johns *et al.*, 2002]. Therefore, a simple shift in the wind field in the subtropics to the south by only 2.5 degrees from their present latitude would, all else being equal, increase the Sverdrup transport at latitude of the Windward Passage by about 4 Sv. This would result in a 4 Sv increase in the wind-driven flow entering the Caribbean and ultimately exiting through the Florida Straits.

[22] Interestingly, during the Little Ice Age a southward migration of the ITCZ has also been inferred [Haug *et al.*, 2001; Lund and Curry, 2006]. However, at this time there appears to be a smaller density gradient across the Florida Straits which all else being equal would imply a lower transport [Lund, 2005]. So the link between ITCZ position

and Florida Straits transport that we see over the last 8 ka will not necessarily extend to other timescales where the forcing and patterns of climate anomalies may be different.

### 3.2.2. Other Changes in Atmospheric Circulation

[23] While the increase in the flow over the course of the Holocene seems consistent in sense and magnitude with a southward migration of the ITCZ, this is not the only possible explanation of the data. Other changes in the wind field could have resulted in the flow increase. For example, most of the coupled models that participated in the PMIP2 project show a more positive North Atlantic Oscillation (NAO) at 6 ka B.P. relative to the modern day, consistent with interpretations of paleoclimate data for this time period [Gladstone *et al.*, 2005]. Renssen *et al.* [2005] also find that in their model study the Arctic Oscillation (AO) index, which is closely related to the NAO, decreases over the Holocene. Baringer and Larsen [2001] find that interannual variations (on the order of 4 Sv) in Florida Straits transport show a strong negative correlation with the North Atlantic Oscillation (NAO) index. So it is possible that the increase in flow is related to the Holocene trend in the AO/NAO and the associated wind patterns.

[24] Attribution of the observed changes in the Florida Current to changes in atmospheric circulation is consistent with the fact that the inferred flow increase is largely driven by the decrease in  $\delta^{18}\text{O}$  (corresponding to decrease in density) of the cores bathed by subtropical mode water on the Bahamas profile (Figure 3).

### 3.2.3. Changes in AMOC

[25] We must also consider the possibility that an increase in Florida Straits transport resulted from an increase in the large-scale meridional overturning circulation associated with NADW export over the last 8 ka. However, climate models show very little change in the overall strength of AMOC in response to the changes of insolation over the Holocene [Otto-Bliesner *et al.*, 2006; Renssen *et al.*, 2005], and there is no deep ocean data suggesting a gradual increase in AMOC over the Holocene.

[26] There have been suggestions of a stronger (or more northward penetrating) North Atlantic Current during the Early Holocene, possibly associated with an enhanced AMOC. However, the warmth seems most pronounced between 8 and 10 ka B.P., before the time interval covered in this study [Hald *et al.*, 2007; Koç *et al.*, 1993]. In addition, Renssen *et al.* [2005] find that much of the data suggesting early Holocene warmth in the far North Atlantic is consistent with the modeled response to changes in external forcing over the course of the Holocene. Their model does show a decrease in deepwater formation in the Nordic Seas over the Holocene, but this is compensated for by an increase in Labrador Sea Deep Water, resulting in very little change in the strength of the AMOC at 20°S. This would imply little change in the

contribution of the surface branch of the AMOC to Florida Straits transport.

[27] On the basis of the carbon isotopes of benthic foraminifera at 2 km water depth in the North Atlantic, Oppo *et al.* [2003] suggest a reduced presence of NADW at around 5 ka and 3 ka B.P. Keigwin *et al.* [2005] observe a similar reduction of benthic  $\delta^{13}\text{C}$  at 5 ka B.P. in a core at 3900 m water depth, but are cautious about interpreting their results as a diminished NADW contribution because of conflicting signals between the Cd/Ca nutrient tracer and benthic  $\delta^{13}\text{C}$  in the same core. If these benthic  $\delta^{13}\text{C}$  values resulted from a diminished export of NADW, we might expect the surface branch of the large-scale overturning circulation which passes through the Florida Straits to weaken as well [Lynch-Stieglitz *et al.*, 1999b]. However, we do not observe a dramatic weakening of the Florida Current at these times. While our 1000 year averaging and dating uncertainty has the potential to smooth out shorter-timescale variability, there is no indication of any systematic deviations around these time periods in benthic  $\delta^{18}\text{O}$  values in the measurements from each core (see Figures S1–S20).

## 4. Conclusions

[28] The contrast in the oxygen isotope ratios in benthic foraminifera on either side of the Florida Current shows an increase over the last 8 ka. Assuming that the relationship between density and the  $\delta^{18}\text{O}$  of foraminifera was the same as today between 0 and 6 ka, and that it changed in a predictable way because of changing ice volume between 6 and 8 ka, this represents an increase in the density contrast across the current, and an increase in the vertical shear of the geostrophic transport. Assuming no changes in the reference level, this density change corresponds to an increase in flow of about 4 Sv over the last 8 ka. We think the simplest explanation for these data is a change in atmospheric circulation and the wind-driven flow of the upper ocean. While many scenarios are possible, a small southward shift of the Atlantic ITCZ could easily account for a flow increase of 4 Sv. There is no evidence for a shutdown or dramatic weakening of the AMOC over the last 8 ka on the time-scales this study can resolve. This reconstruction suggests a relatively robust Atlantic MOC for the mid- to late Holocene, and provides a backdrop against which to compare the magnitude of future changes which could occur in response to increased greenhouse gases.

[29] **Acknowledgments.** This work was supported by NSF grants OCE-9984989/OCE-0428803 and OCE-0096472 to J.L.-S. and NSF grants OCE-0096469 to W.B.C. We thank the editor and two anonymous reviewers for helpful suggestions on the manuscript. We thank L. Baker, J. Broda, T. Chiang, H. Griffiths, and D. Ostermann for their technical assistance. We also thank the officers and crew of the R/V *Knorr* for their contributions to the field program.

## References

- Andersen, K. K., *et al.* (2004), High-resolution record of Northern Hemisphere climate extending into the last interglacial period, *Nature*, 431(7005), 147–151, doi:10.1038/nature02805.
- Baringer, M. O., and J. C. Larsen (2001), Sixteen years of Florida Current transport at 27°N, *Geophys. Res. Lett.*, 28(16), 3179–3182, doi:10.1029/2001GL013246.
- Bé, A. W. H. (1980), Gametogenic calcification in a spinose planktonic foraminifer, *Globigerinoides sacculifer* (Brady), *Mar. Micropaleontol.*, 5, 283–310, doi:10.1016/0377-8398(80)90014-6.

- Bond, G., et al. (2001), Persistent solar influence on North Atlantic climate during the Holocene, *Science*, 294(5549), 2130–2136, doi:10.1126/science.1065680.
- Braconnot, P., et al. (2007), Results of PMIP2 coupled simulations of the mid-Holocene and Last Glacial Maximum—Part 2: Feedbacks with emphasis on the location of the ITCZ and mid- and high latitudes heat budget, *Clim. Past*, 3(2), 279–296.
- Broccoli, A. J., K. A. Dahl, and R. J. Stouffer (2006), Response of the ITCZ to Northern Hemisphere cooling, *Geophys. Res. Lett.*, 33, L01702, doi:10.1029/2005GL024546.
- Came, R. E., W. B. Curry, D. W. Oppo, A. J. Broccoli, R. J. Stouffer, and J. Lynch-Stieglitz (2007), North Atlantic intermediate depth variability during the Younger Dryas: Evidence from benthic foraminiferal Mg/Ca and the GFDL R30 coupled climate model, in *Ocean Circulation: Mechanisms and Impacts—Past and Future Changes of Meridional Overturning*, *Geophys. Monogr. Ser.*, vol. 173, edited by A. Schmittner, J. Chiang, and S. Hemmings, pp. 247–263, AGU, Washington, D. C.
- Craig, H., and L. I. Gordon (1965), Deuterium and oxygen 18 variations in the ocean and the marine atmosphere: Stable isotopes in oceanographic studies and paleotemperatures, in *Proceedings of the Third Spoleto Conference: Spoleto, Italy*, edited by E. Tongioli, pp. 9–130, Sischì and Figli, Pisa, Italy.
- deMenocal, P., et al. (2000), Coherent high- and low-latitude climate variability during the Holocene warm period, *Science*, 288(5474), 2198–2202.
- Deuser, W. G., and E. H. Ross (1989), Seasonally abundant planktonic foraminifera of the Sargasso Sea: Succession, deep-water fluxes, isotopic composition and paleoceanographic implications, *J. Foraminiferal Res.*, 19, 268–293.
- Gasse, F. (2000), Hydrological changes in the African tropics since the Last Glacial Maximum, *Quat. Sci. Rev.*, 19(1–5), 189–211.
- Gladstone, R. M., et al. (2005), Mid-Holocene NAO: A PMIP2 model intercomparison, *Geophys. Res. Lett.*, 32, L16707, doi:10.1029/2005GL023596.
- González, N. M., F. E. Müller-Karger, S. C. Estrada, R. Pérez de los Reyes, I. V. del Río, P. C. Pérez, and I. M. Arenal (2000), Near-surface phytoplankton distribution in the western Intra-Americas Sea: The influence of El Niño and weather events, *J. Geophys. Res.*, 105(C6), 14,029–14,043, doi:10.1029/2000JC900017.
- Hald, M., et al. (2007), Variations in temperature and extent of Atlantic water in the northern North Atlantic during the Holocene, *Quat. Sci. Rev.*, 26(25–28), 3423–3440, doi:10.1016/j.quascirev.2007.10.005.
- Hall, I. R., et al. (2004), Centennial to millennial scale Holocene climate-deep water linkage in the North Atlantic, *Quat. Sci. Rev.*, 23(14–15), 1529–1536, doi:10.1016/j.quascirev.2004.04.004.
- Haug, G. H., et al. (2001), Southward migration of the intertropical convergence zone through the Holocene, *Science*, 293(5533), 1304–1308, doi:10.1126/science.1059725.
- Hoelzmann, P., D. Jolly, S. P. Harrison, F. Laarif, R. Bonnefille, H.-J. Pachur, and TEMPO (1998), Mid-Holocene land-surface conditions in northern Africa and the Arabian Peninsula: A data set for the analysis of biogeophysical feedbacks in the climate system, *Global Biogeochem. Cycles*, 12(1), 35–51, doi:10.1029/97GB02733.
- Hughen, K. A., et al. (2004), Marine04 marine radiocarbon age calibration, 0–26 cal kyr BP, *Radiocarbon*, 46(3), 1059–1086.
- Johns, W. E., et al. (2002), On the Atlantic inflow to the Caribbean Sea, *Deep Sea Res., Part I*, 49, 1307, doi:10.1016/S0967-0637(02)00026-2.
- Kara, A. B., et al. (2002), Naval Research Laboratory mixed layer depth (NMLD) climatologies, *Rep. NRL/FR/7330-02-9995*, 26 pp., Naval Res. Lab., Washington, D. C.
- Kaufman, D. S., et al. (2004), Holocene thermal maximum in the western Arctic (0–180°W), *Quat. Sci. Rev.*, 23(5–6), 529–560, doi:10.1016/j.quascirev.2003.09.007.
- Keigwin, L. D., J. P. Sachs, Y. Rosenthal, and E. A. Boyle (2005), The 8200 year B. P. event in the slope water system, western sub-polar North Atlantic, *Paleoceanography*, 20, PA2003, doi:10.1029/2004PA001074.
- Kerwin, M. W., J. T. Overpeck, R. S. Webb, A. DeVernal, D. H. Rind, and R. J. Healy (1999), The role of oceanic forcing in mid-Holocene Northern Hemisphere climatic change, *Paleoceanography*, 14(2), 200–210, doi:10.1029/1998PA900011.
- Koc, N., E. Jansen, and H. Hafliðason (1993), Paleocceanographic reconstructions of surface ocean conditions in the Greenland, Iceland and Norwegian seas through the last 14 ka based on diatoms, *Quat. Sci. Rev.*, 12(2), 115–140, doi:10.1016/0277-3791(93)90012-B.
- Lambeck, K., and J. Chappell (2001), Sea level change through the last glacial cycle, *Science*, 292(5517), 679–686, doi:10.1126/science.1059549.
- Leaman, K. D., et al. (1989), The average distribution of volume transport and potential vorticity with temperature at three sections across the Gulf Stream, *J. Phys. Oceanogr.*, 19(1), 36–51, doi:10.1175/1520-0485(1989)019<0036:TADOVT>2.0.CO;2.
- Leaman, K. D., P. S. Vertes, L. P. Atkinson, T. N. Lee, P. Hamilton, and E. Waddell (1995), Transport, potential vorticity, and current/temperature structure across Northwest Providence and Santaren channels and the Florida Current off Cay Sal Bank, *J. Geophys. Res.*, 100(C5), 8561–8569, doi:10.1029/94JC01436.
- Lee, T. N., et al. (1996), Moored observations of western boundary current variability and thermohaline circulation at 26.5°N in the subtropical North Atlantic, *J. Phys. Oceanogr.*, 26, 962–983.
- Lund, D. C. (2005), Gulf Stream temperature, salinity, and transport during the last millennium, Ph.D. thesis, Mass. Inst. of Technol., Cambridge.
- Lund, D. C., and W. Curry (2006), Florida Current surface temperature and salinity variability during the last millennium, *Paleoceanography*, 21, PA2009, doi:10.1029/2005PA001218.
- Lund, D. C., et al. (2006), Gulf Stream density structure and transport during the past millennium, *Nature*, 444(7119), 601–604, doi:10.1038/nature05277.
- Lynch-Stieglitz, J., W. B. Curry, and N. Slowey (1999a), A geostrophic transport estimate for the Florida Current from the oxygen isotope composition of benthic foraminifera, *Paleoceanography*, 14(3), 360–373, doi:10.1029/1999PA900001.
- Lynch-Stieglitz, J., et al. (1999b), Weaker Gulf Stream in the Florida Straits during the Last Glacial Maximum, *Nature*, 402(6762), 644–648, doi:10.1038/45204.
- Marchal, O., et al. (2002), Apparent long-term cooling of the sea surface in the northeast Atlantic and Mediterranean during the Holocene, *Quat. Sci. Rev.*, 21(4–6), 455–483, doi:10.1016/S0277-3791(01)00105-6.
- Oppo, D. W., et al. (2003), Palaeo-oceanography: Deepwater variability in the Holocene epoch, *Nature*, 422(6929), 277–278, doi:10.1038/422277b.
- Otto-Bliesner, B. L., et al. (2006), Last Glacial Maximum and Holocene climate in CCSM3, *J. Clim.*, 19, 2526–2544, doi:10.1175/JCLI3748.1.
- Renssen, H., et al. (2005), Simulating the Holocene climate evolution at northern high latitudes using a coupled atmosphere-sea ice-ocean-vegetation model, *Clim. Dyn.*, 24(1), 23–43, doi:10.1007/s00382-004-0485-y.
- Schmitz, W. J., and P. L. Richardson (1991), On the sources of the Florida Current, *Deep Sea Res., Part A*, 38, S379–S409.
- Schmitz, W. J., Jr., J. D. Thompson, and J. R. Luyten (1992), The Sverdrup circulation for the Atlantic along 24°N, *J. Geophys. Res.*, 97, 7251–7256, doi:10.1029/92JC00417.
- Schrag, D. P., et al. (2002), The oxygen isotopic composition of seawater during the Last Glacial Maximum, *Quat. Sci. Rev.*, 21(1–3), 331–342, doi:10.1016/S0277-3791(01)00110-X.
- Slowey, N. C., and W. B. Curry (1995), Glacial-interglacial differences in circulation and carbon cycling within the upper western North Atlantic, *Paleoceanography*, 10(4), 715–732, doi:10.1029/95PA01166.

W. B. Curry, Woods Hole Oceanographic Institution, Woods Hole, MA 02543, USA.

D. C. Lund, Department of Geological Sciences, University of Michigan, Ann Arbor, MI 48109, USA.

J. Lynch-Stieglitz, School of Earth and Environmental Sciences, Georgia Institute of Technology, 311 Ferst Drive, Atlanta, GA 30332, USA. (jean@eas.gatech.edu)